


***In Situ* Observation of Hall Magnetohydrodynamic Cascade in Space Plasma**Riddhi Bandyopadhyay *Department of Physics and Astronomy, University of Delaware, Newark, Delaware 19716, USA*Luca Sorriso-Valvo *Departamento de Física, Escuela Politécnica Nacional, 170517 Quito, Ecuador
and Istituto per la Scienza e Tecnologia dei Plasmi, Consiglio Nazionale delle Ricerche, 87036 Bari, Italy*Alexandros Chasapis *Laboratory for Atmospheric and Space Physics, University of Colorado Boulder,
Boulder, Colorado 80303, USA*Petr Hellinger *Astronomical Institute, CAS, Bocni II/1401, CZ-14100 Prague, Czech Republic
and Institute of Atmospheric Physics, CAS, Bocni II/1401, CZ-14100 Prague, Czech Republic*William H. Matthaeus **Department of Physics and Astronomy, University of Delaware, Newark, Delaware 19716, USA
and Bartol Research Institute, University of Delaware, Newark, Delaware 19716, USA*

Andrea Verdini and Simone Landi

*Dipartimento di Fisica e Astronomia, Università degli Studi di Firenze, 50125 Firenze, Italy
and INAF, Osservatorio Astrofisico di Arcetri, Largo E. Fermi 5, I-50125 Firenze, Italy*

Luca Franci

*School of Physics and Astronomy, Queen Mary University of London, London E1 4NS, United Kingdom
and INAF, Osservatorio Astrofisico di Arcetri, Largo E. Fermi 5, I-50125 Firenze, Italy*Lorenzo Matteini †*LESIA, Observatoire de Paris, Meudon, France
and INAF, Osservatorio Astrofisico di Arcetri, Largo E. Fermi 5, I-50125 Firenze, Italy*Barbara L. Giles , Daniel J. Gershman, and Thomas E. Moore
NASA Goddard Space Flight Center, Greenbelt, Maryland 20771, USA

Craig J. Pollock

*Denali Scientific, Fairbanks, Alaska 99709, USA*Christopher T. Russell  and Robert J. Strangeway *University of California, Los Angeles, California 90095-1567, USA*

Roy B. Torbert

*University of New Hampshire, Durham, New Hampshire 03824, USA*James L. Burch *Southwest Research Institute, San Antonio, Texas 78238-5166, USA*

(Received 12 July 2019; revised manuscript received 7 April 2020; accepted 1 May 2020; published 4 June 2020)

We present estimates of the turbulent energy-cascade rate derived from a Hall-magnetohydrodynamic (MHD) third-order law. We compute the contribution from the Hall term and the MHD term to the energy flux. Magnetospheric Multiscale (MMS) data accumulated in the magnetosheath and the solar wind are compared with previously established simulation results. Consistent with the simulations, we find that at large (MHD) scales, the MMS observations exhibit a clear inertial range dominated by the MHD flux. In the subion range, the cascade continues at a diminished level via the Hall term, and the change becomes

more pronounced as the plasma beta increases. Additionally, the MHD contribution to interscale energy transfer remains important at smaller scales than previously thought. Possible reasons are offered for this unanticipated result.

DOI: 10.1103/PhysRevLett.124.225101

Fully developed turbulence is characterized by scale-invariant energy transfer across the inertial range of length scales, where nonlinear terms dominate the dynamics [1]. In the solar wind, planetary magnetospheres, and other turbulent astrophysical plasmas, large-scale energy, in the form of velocity shears and electromagnetic fluctuations, is transferred across scales and dissipated at small scales. This process is known as *energy cascade*. Turbulent energy cascade and dissipation have important effects in space and astrophysical systems and are considered an important source for the observed plasma heating [2] and acceleration of energetic particles.

In homogeneous, neutral fluid turbulence, the Kolmogorov-Yaglom law [3,4] quantifies the mean energy dissipation rate in terms of longitudinal, third-order structure functions. The Kolmogorov-Yaglom third-order law is extended to the case of plasmas in the incompressible magnetohydrodynamic (MHD) description by Politano and Pouquet [5,6] and Politano and co-workers [7]. This MHD theory accounts for the *incompressible channel* of the inertial-range energy cascade. For plasmas with small density fluctuations, such as the cases presented here, the incompressible transfer is expected to contribute a majority of the total energy transfer [8–10].

In the rapid streaming of the solar wind (at mean speed $\langle \mathbf{V} \rangle$), the Taylor hypothesis [11] ($\mathbf{r} = t\langle \mathbf{V} \rangle$) permits the conversion of space (\mathbf{r}) and time (t) arguments. Then, the Politano-Pouquet law prescribes the linear scaling of the mixed, third-order moment

$$Y(\ell) \equiv \langle \delta v_l (|\delta \mathbf{v}|^2 + |\delta \mathbf{b}|^2) - 2\delta b_l (\delta \mathbf{v} \cdot \delta \mathbf{b}) \rangle = -\frac{4}{3} \varepsilon \ell, \quad (1)$$

where δ indicates an increment, e.g., $\delta \psi(t, \delta t) = \psi(t + \delta t) - \psi(t)$ for a generic field ψ and $\ell = \delta t \langle V \rangle$. In MHD, we compute increments of the plasma velocity \mathbf{v} or the magnetic field $\mathbf{b} = \mathbf{B} / \sqrt{4\pi\rho}$ (in Alfvén units, mass density ρ) using a temporal lag δt . The subscript l indicates longitudinal components, and ε is the mean energy-transfer rate.

Assuming that the turbulence is approximately statistically stationary and homogeneous [12], Eq. (1) enables the estimation of the fluid-scale energy-transfer rate. The Politano-Pouquet law, in its isotropic form, has been verified in solar-wind studies [13–16], and more recently in the terrestrial magnetosheath [9,17] and magnetospheric boundary layer [18]. The cascade rate measured this way is shown to sufficiently account for the solar-wind heating [19–21]. The presence of a significant mean magnetic field in the solar wind leads to an expectation of spectral anisotropy [22].

However, even when the anisotropic form of the Politano-Pouquet law is used to derive the solar-wind heating rate, the results are fairly close to that obtained from the isotropic scaling law [23,24].

The single-fluid MHD phenomenology is only suitable in the fluid regime—large length scales and low frequencies. As smaller length scales are approached near the ion gyroradius (ρ_i) or ion-inertial length (d_i), the nature of the cascade is expected to change. For example, ideal motions of the plasma should render the magnetic field “frozen in” the electron fluid motions at velocity \mathbf{v}_e , rather than frozen into the MHD fluid frame at (proton) velocity \mathbf{v} . Near the kinetic scales, to first-order approximation, kinetic physics can be partially included via the Hall electric field in the fluid model [25]. Accordingly, employing the equations of incompressible Hall MHD, a scaling law for the third-order structure functions analogous to its MHD counterpart can be derived to obtain the energy-cascade flux at the scale of interest [26–28]. In the Hall-MHD formulation, the third-order moment scaling law includes the additional Hall term

$$H(\ell) \equiv \langle 2\delta b_l (\delta \mathbf{b} \cdot \delta \mathbf{j}) - \delta j_l |\delta \mathbf{b}|^2 \rangle. \quad (2)$$

Here, \mathbf{j} is the electric current density in Alfvén units $\mathbf{j} = \mathbf{v} - \mathbf{v}_e$, where \mathbf{v} is the proton velocity and \mathbf{v}_e is the electron velocity. When the displacement current is neglected, this is equivalent to $\mathbf{j} = \nabla \times \mathbf{b}$. Hellinger *et al.* [27] derive the Hall contribution as H , neglecting an additional contribution equal to $-H/2$ [28], so that the complete scaling law reads

$$Y + \frac{1}{2}H = -\frac{4}{3} \varepsilon \ell. \quad (3)$$

In applying this equation to spacecraft observations in a weakly collisional plasma, as we do here, or to simulations as in Ref. [27], we recognize that such a formulation is incomplete and lacks many kinetic effects. However, in general one expects that such additional effects will be additive, and therefore, from a theoretical perspective the Hall third-order law represents a better measure of the energy-transfer rate near the kinetic scales, compared to MHD. The linear scaling Eq. (3) has been recently applied to hybrid-kinetic numerical simulations [27,28], where the Hall-MHD-generalized flux becomes dominant at small scales, continuing a scale-invariant cascade further into the subproton range. However, the energy-cascade flux decreases near the kinetic scale, even after including the contribution from the Hall term. This decrease is stronger in high- β plasma.

TABLE I. Some plasma parameters of the selected intervals. SW (solar wind), MSH (magnetosheath).

Interval	β_i	$ \langle \mathbf{B} \rangle $ (nT)	$B_{\text{rms}}/ \langle \mathbf{B} \rangle $	$\rho_{\text{rms}}/\langle \rho \rangle$	M_t	$ \langle \mathbf{V} \rangle $ (km s ⁻¹)	V_A (km s ⁻¹)	d_i (km)	L_{corr} (km)
SW	0.4 ^a	7.4	0.3	0.08	0.3 ^a	330	51	75	11×10^4
MSH	17	3.4	2.5	0.2	0.2	278	18	56	1350

^aTemperature provided by Wind [35,36] spacecraft is used to compute the beta value and the turbulent Mach number in the solar wind.

In this work, we study the Hall-MHD third-order law using *in situ* data from the Magnetospheric Multiscale (MMS) spacecraft [29–31] and compare the results directly with the analysis of two-dimensional hybrid-kinetic numerical simulations [27]. The MMS results exhibit similarities to and, perhaps surprisingly, some contrasts with, the simulation results and baseline theoretical expectations.

To study the Hall-MHD third-order law, we use burst resolution MMS data accumulated in two distinct turbulent plasma environments. The first one is an hour-long solar-wind (SW) interval on November 26, 2017 from 21:09:03 to 22:09:03 UTC, far from Earth’s bow shock. We do not find any signature of reflected ions from the bow shock, so the solar-wind interval can be considered to be “pristine.”

The second dataset that we use is a MMS interval sampled in the terrestrial magnetosheath (MSH) on October 27, 2018 from 09:13:13 to 09:57:43 UTC. Here, the plasma beta is much higher with an average value of $\beta_i = 17$. Table I reports some important plasma parameters for the two selected intervals. From Table I, we note that for the chosen intervals, the flow speed is larger than the Alfvén speed, indicating that the Taylor hypothesis is expected to be valid. These MMS intervals are typical—analyses of other solar-wind and magnetosheath samples (not shown, but see Supplemental Material [32]) exhibit similar properties and conclusions (also see Refs. [9,33,34]).

Figure 1 illustrates the power spectral density (PSD) of the magnetic field fluctuations for the two chosen intervals plotted against kd_i . The level of fluctuations is considerably higher in the magnetosheath interval than in the solar wind. Both spectra exhibit Kolmogorov-like $-5/3$ scaling in the inertial range followed by a steepening near $kd_i = 1$. However, the solar-wind spectrum has a significantly broader bandwidth of inertial range, representative of a larger and higher Reynolds number system, compared to the magnetosheath interval [33,34].

Having shown that the two chosen intervals exhibit extended, inertial-range Kolmogorov spectra, we compute the energy flux from Eq. (3). The required electron and proton moments provided by the fast plasma investigation (FPI) instrument in the solar wind, are processed using the method described in Ref. [37] to exclude instrumental artifacts that arise when FPI operates in the solar wind. All analyses are performed over the four MMS spacecraft and then averaged. In the solar wind, a spintone signal is

introduced likely due to issues in the very low-energy response of the electrons, and a systematic offset in the ion and electron velocities. Therefore, we use the curlometer-based [38] current for the Hall term.

Figure 2 shows the scaling of the third-order structure functions decomposed into the MHD ($-Y$) and Hall-MHD ($-H/2$) terms from Eq. (3) with spatial lag in units of d_i . Only parts of the structure functions that lie well above the instrumental noise level are plotted here. A roughly linear scaling is observed in the inertial range for both samples. In both samples, the MHD component $-Y$ shows better scaling in the inertial range, where it is dominant with respect to the Hall term $-H/2$. The latter has more defined scaling at scales near or below d_i , where its contribution to the energy transfer becomes of the same order as for the MHD term. Note that although the structure functions exhibit large fluctuations at scales near and larger than the correlation scale, within the narrow range demarcated by vertical dashed and solid lines the linear scaling is rather satisfactory and smooth (Fig. 2, bottom panel).

In order to compare the above results with numerical simulations, we use two different two-dimensional runs of the hybrid code CAMELIA [39]. The two runs have $\beta_i = 0.5$ and 8, respectively, chosen to probe variations of β comparable to the contrast in the solar-wind and magnetosheath plasma properties. The simulation box has the size

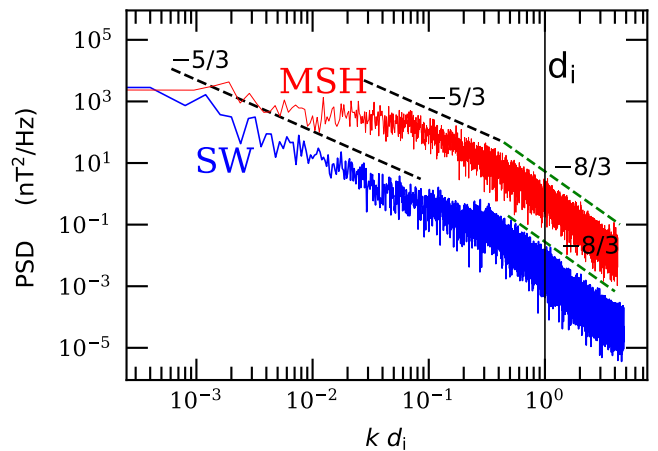


FIG. 1. Magnetic field spectra for the solar-wind (SW, in blue) and magnetosheath (MSH, in red) interval. The solid vertical line represents $kd_i = 1$ with the wave vector $k \simeq (2\pi f)/|\langle \mathbf{V} \rangle|$, where f is the frequency.

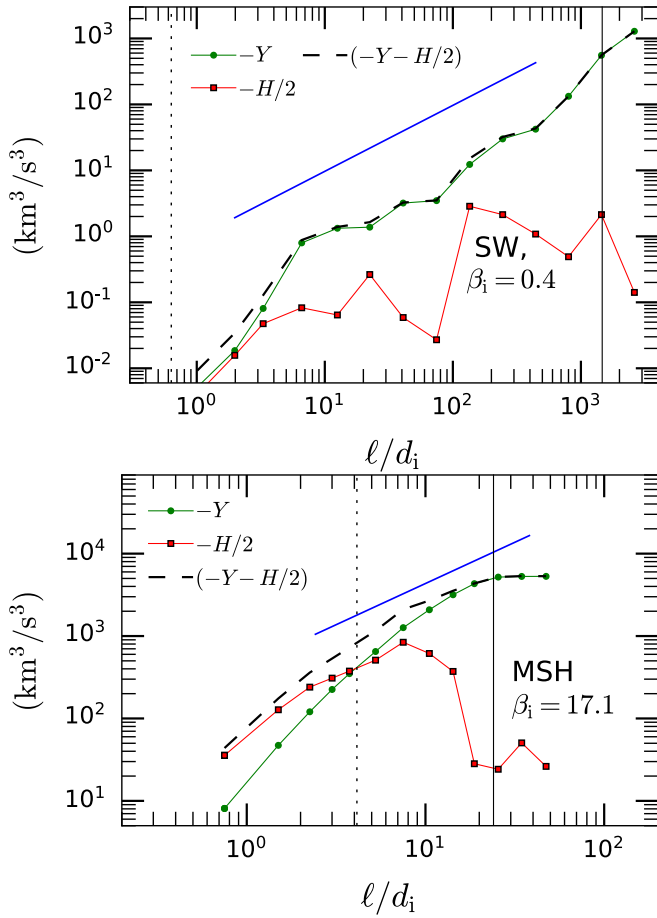


FIG. 2. MHD ($-Y$) and Hall ($-H/2$) structure function from generalized third-order law [Eq. (3)] from MMS data. Top: solar wind, $\beta_i = 0.4$. Bottom: magnetosheath, $\beta_i = 17.1$. The proton gyroradius ρ_i is shown as a dotted vertical line, and the correlation length L_{corr} is shown as a solid vertical line. A linear scaling with arbitrary offset is shown for reference.

$256d_i \times 256d_i$ for both runs. A more detailed description of these runs can be found in Refs. [27,40].

Figure 3 shows the Hall-MHD third-order law (3) [28] in Alfvén speed units, in a format similar to Fig. 2. The transition between the MHD and ion (or Hall) scales occurs roughly at the ion gyroradius ρ_i , which is indicated by the dotted vertical line. The correlation length is about $10d_i$ for both runs, and it is indicated by solid black vertical line. The relatively small range of linear scaling seen in the simulation results is typical of hybrid simulation [41], and due to limits on available computing resources, it is an unavoidable consequence of limited scale and resolution. However, there is a reasonable level of qualitative agreement with the observations. In particular, in the low- β simulation the Hall term $-H/2$ becomes relevant closer to the transition scale more prominently than in the high- β case. Conversely, the dominance of the MHD contribution is established more dramatically at larger scales in the lower- β solar wind and lower-beta simulation. Note that

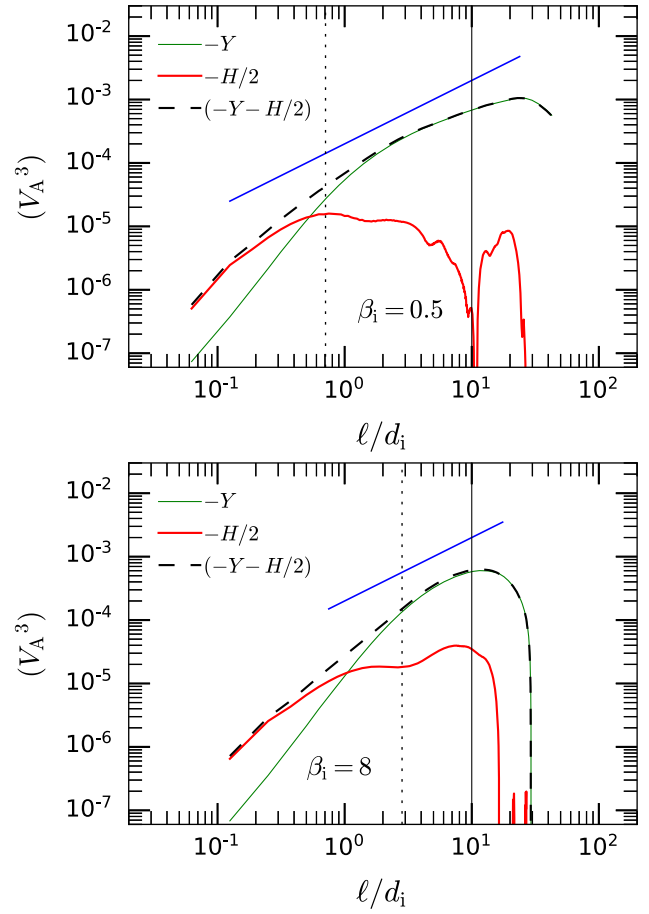


FIG. 3. MHD ($-Y$) and Hall ($-H/2$) structure function from generalized third-order law [Eq. (3)] from 2D hybrid-kinetic simulations. Top panel: $\beta_i = 0.5$. Bottom panel: $\beta_i = 8$. The dotted vertical line indicates the ion gyroradius ρ_i , and the solid vertical line indicates the correlation length L_{corr} . A linear scaling with arbitrary offset is shown for reference.

these include a corrected Hall-term contribution relative to earlier results [27].

While the observational results behave qualitatively similar to the simulations near the kinetic scales and at larger scales, the comparison in the subproton range of scales is less clear. Unlike in the numerical simulations, in the observations, the Hall-contributed cascade becomes significant at much larger scale and the MHD-contributed cascade remains important at smaller scales. Still, in all cases we can confirm that the Hall physics becomes increasingly important for the energy transfer at subproton scales. However, both simulation and *in situ* observations have implicit limitations that may provide a possible explanation for the apparent (if somewhat subtle) differences.

To support the conclusion that the Hall term becomes significant at larger scales in observations than in the simulations, we analyze a few more simulation and MMS datasets (see Supplemental Material [32]) with a wide range of β_i values. We evaluate the ratio of the MHD

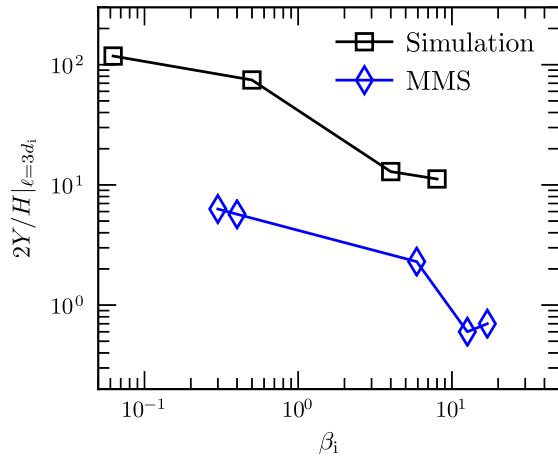


FIG. 4. Variation with ion beta of the ratio of the MHD term ($-Y$) to the Hall-MHD term ($-H/2$) in the third-order cascade rate at lag $\ell = 3d_i$, as obtained from simulation and MMS data.

to the Hall term in Eq. (3) for a fixed length scale of $\ell = 3d_i$, and plot them with the β_i values in Fig. 4. Although both simulations and observations exhibit a decreasing trend with increasing β_i , the ratio is significantly smaller for the observational cases compared to the simulations.

There may be several reasons for this difference. The magnetosheath is a system smaller than the solar wind, and exhibits a significantly narrower range between kinetic scale (either ρ_i or d_i) and the correlation scale. It is possible that the small separation of scales does not allow the two contributions to the energy flux to be sufficiently distinct [42]. Deviation from strict statistical homogeneity and incompressibility may also play a role. A notable feature is that, in both magnetosheath and solar-wind cases, the Hall and standard-MHD cascade contributions (Fig. 2) become comparable at a few d_i , at nearly the scales where the corresponding kinetic range modifications [43] to the spectra begin to be seen (Fig. 1). In the simulations, the more dramatic crossover of Hall and MHD effects occurs at moderately smaller sub- d_i scales.

At the same time, the hybrid-kinetic simulations are two dimensional and admit rather low Reynolds number values, both of which may potentially alter the nature of the energy cascade. Additionally, the hybrid simulations ignore the kinetic effects of electrons. With the current computational ability, three-dimensional hybrid simulations would be severely limited in Reynolds number, even more so in full kinetic simulations. For these reasons, a precise quantitative correspondence between the observations and currently attainable simulations should not be expected.

Finally, Table II reports the approximate values of the inertial-range energy-transfer rate obtained for the two chosen intervals from the Hall-MHD scaling law [Eq. (3)]. The second column denotes the total energy-transfer rate from the Hall-MHD law: $\epsilon_{\text{inertial}} = -3(Y + H/2)/4\ell$. The

TABLE II. Energy flux in units of $\text{J kg}^{-1} \text{s}^{-1}$.

Interval	$\epsilon_{\text{inertial}}$	ϵ_{vK}
SW	$(0.9 \pm 0.1) \times 10^3$	0.7×10^3
MSH	$(3 \pm 0.5) \times 10^6$	2.6×10^6

magnetosheath energy-decay rate is about 3 orders of magnitude larger than the interplanetary solar wind [9,17,18]. The final column is a rough estimate of the global energy decay rate at the energy-containing scale obtained from a von Kármán–Taylor [3,44–46] phenomenology (see Ref. [17] and the Supplemental Material [32]). The von Kármán estimates are close to the inertial-scale ones from the third-order law. Although the energy-cascade flux has a fairly constant value in the inertial range, all the MMS intervals as well as the current and prior simulations [27] indicate that the flux on average decreases near the kinetic scales, even after including the Hall contribution. This decrease is more prominent in the high-beta cases, and presumably is due to the onset of other kinetic effects at subproton scales [47]. Note that the value of the proton beta does not affect the cascade rate, which is determined by the energy budget at the large scales, as estimated by the von Kármán theory.

Understanding how collisionless plasmas dissipate remains a topic of central importance in space physics, astrophysics, and laboratory plasma. In recent years, it has become increasingly recognized that the MHD description must be refined to clearly make a connection with kinetic plasma dissipation. The present results provide a step toward understanding this problem. Based on the unprecedented capabilities of the MMS mission instrumentation, the findings of this Letter confirm the applicability of the Hall-modified third-order order laws to describe the physics of transition to kinetic effects near proton scales. We note that a similar paper has recently been published [48], with results in the magnetosheath, while in the present work we also analyze solar-wind results and compare them with simulations. We may summarize by saying that the trend in relative strength of the Hall effect on the cascade is confirmed in the observations and simulations, with respect to variation of beta and scale. However, the disparity in magnitude of both effects differs, presumably due to the effects described above. This raises a note of caution with regard to quantitative comparisons with observations due to limiting approximations of several types. Clarification of these subtle differences awaits investigations with more advanced simulations and observational data when available in the future.

All MMS data are available at Ref. [49]. The Wind data, shifted to Earth’s bow-shock nose, can be found at [50].

A. C. is supported in part by the Magnetospheric Multiscale FIELDS project and in part by National Aeronautics and Space Administration Grant No. 80NSSC19K1469. L. S. V. is supported by the Escuela Politécnica Nacional Internal

Project No. PII-DFIS-2019-01. W. H. M. is a member of the Magnetospheric Multiscale Theory and Modeling team and is supported by NASA Grants No. NNX14AC39G and No. 80NSSC19K0565, and NASA Supporting Research Grant No. NNX17AB79G. P.H. acknowledges Grant No. 18-08861S from the Czech Science Foundation. We are grateful to the MMS instrument teams for cooperation and collaboration in preparing the data. The data used in this analysis are Level 2 FIELDS and FPI data products, in cooperation with the instrument teams and in accordance with their guidelines. The authors thank the Wind team for the magnetic field and proton moment dataset.

*Corresponding author.

whm@udel.edu

†Present address: Physics Department, Imperial College London, London SW7 2AZ, United Kingdom.

- [1] A. N. Kolmogorov, C. R. Acad. Sci. URSS **32**, 16 (1941); Reprinted in Proc. R. Soc. A **434**, 15 (1991).
- [2] J. D. Richardson, K. I. Paularena, A. J. Lazarus, and J. W. Belcher, *Geophys. Res. Lett.* **22**, 325 (1995).
- [3] T. de Kármán and L. Howarth, Proc. R. Soc. A **164**, 192 (1938).
- [4] A. N. Kolmogorov, Dokl. Akad. Nauk SSSR **30**, 301 (1941); Reprinted in Proc. R. Soc. A **434**, 9 (1991).
- [5] H. Politano and A. Pouquet, *Geophys. Res. Lett.* **25**, 273 (1998).
- [6] H. Politano and A. Pouquet, *Phys. Rev. E* **57**, R21 (1998).
- [7] L. Sorriso-Valvo, V. Carbone, A. Noullez, H. Politano, A. Pouquet, and P. Veltri, *Phys. Plasmas* **9**, 89 (2002).
- [8] Y. Yang, W. H. Matthaeus, Y. Shi, M. Wan, and S. Chen, *Phys. Fluids* **29**, 035105 (2017).
- [9] L. Z. Hadid, F. Sahraoui, S. Galtier, and S. Y. Huang, *Phys. Rev. Lett.* **120**, 055102 (2018).
- [10] V. Montagud-Camps, R. Grappin, and A. Verdini, *Astrophys. J.* **853**, 153 (2018).
- [11] G. I. Taylor, Proc. R. Soc. A **164**, 476 (1938).
- [12] W. H. Matthaeus and M. L. Goldstein, *J. Geophys. Res.* **87**, 10347 (1982).
- [13] B. T. MacBride, M. A. Forman, and C. W. Smith, in *Proceedings of Solar Wind 11/SOHO 16, Connecting Sun and Heliosphere*, edited by B. Fleck, T. H. Zurbuchen, and H. Lacoste (European Space Agency, 2005), Vol. 592, p. 613, <https://ui.adsabs.harvard.edu/abs/2005ESASP.592..613M>.
- [14] L. Sorriso-Valvo, R. Marino, V. Carbone, A. Noullez, F. Lepreti, P. Veltri, R. Bruno, B. Bavassano, and E. Pietropaolo, *Phys. Rev. Lett.* **99**, 115001 (2007).
- [15] J. T. Coburn, C. W. Smith, B. J. Vasquez, J. E. Stawarz, and M. A. Forman, *Astrophys. J.* **754**, 93 (2012).
- [16] S. Banerjee, L. Z. Hadid, F. Sahraoui, and S. Galtier, *Astrophys. J. Lett.* **829**, L27 (2016).
- [17] R. Bandyopadhyay, A. Chasapis, R. Chhiber, T. N. Parashar, W. H. Matthaeus, M. A. Shay, B. A. Maruca, J. L. Burch, T. E. Moore, C. J. Pollock, B. L. Giles, W. R. Paterson, J. Dorelli, D. J. Gershman, R. B. Torbert, C. T. Russell, and R. J. Strangeway, *Astrophys. J.* **866**, 106 (2018).
- [18] L. Sorriso-Valvo *et al.*, *Phys. Rev. Lett.* **122**, 035102 (2019).
- [19] B. J. Vasquez, C. W. Smith, K. Hamilton, B. T. MacBride, and R. J. Leamon, *J. Geophys. Res.* **112**, A07101 (2007).
- [20] B. T. MacBride, C. W. Smith, and M. A. Forman, *Astrophys. J.* **679**, 1644 (2008).
- [21] R. Marino, L. Sorriso-Valvo, V. Carbone, A. Noullez, R. Bruno, and B. Bavassano, *Astrophys. J.* **677**, L71 (2008).
- [22] J. V. Shebalin, W. H. Matthaeus, and D. Montgomery, *J. Plasma Phys.* **29**, 525 (1983).
- [23] K. T. Osman, M. Wan, W. H. Matthaeus, J. M. Weygand, and S. Dasso, *Phys. Rev. Lett.* **107**, 165001 (2011).
- [24] A. Verdini, R. Grappin, P. Hellinger, S. Landi, and W. C. Müller, *Astrophys. J.* **804**, 119 (2015).
- [25] E. Papini, L. Franci, S. Landi, A. Verdini, L. Matteini, and P. Hellinger, *Astrophys. J.* **870**, 52 (2019).
- [26] S. Galtier, *Phys. Rev. E* **77**, 015302(R) (2008).
- [27] P. Hellinger, A. Verdini, S. Landi, L. Franci, and L. Matteini, *Astrophys. J. Lett.* **857**, L19 (2018).
- [28] R. Ferrand, S. Galtier, F. Sahraoui, R. Meyrand, N. Andrés, and S. Banerjee, *Astrophys. J.* **881**, 50 (2019).
- [29] J. L. Burch, T. E. Moore, R. B. Torbert, and B. L. Giles, *Space Sci. Rev.* **199**, 5 (2016).
- [30] C. Pollock *et al.*, *Space Sci. Rev.* **199**, 331 (2016).
- [31] C. T. Russell *et al.*, *Space Sci. Rev.* **199**, 189 (2016).
- [32] See Supplemental Material at <http://link.aps.org/supplemental/10.1103/PhysRevLett.124.225101>, for similar analyses of a few more MMS intervals and simulations.
- [33] S. Y. Huang, F. Sahraoui, X. H. Deng, J. S. He, Z. G. Yuan, M. Zhou, Y. Pang, and H. S. Fu, *Astrophys. J. Lett.* **789**, L28 (2014).
- [34] S. Y. Huang, L. Z. Hadid, F. Sahraoui, Z. G. Yuan, and X. H. Deng, *Astrophys. J. Lett.* **836**, L10 (2017).
- [35] K. W. Ogilvie, D. J. Chornay, R. J. Fritzenreiter, F. Hunsaker, J. Keller, J. Lobell, G. Miller, J. D. Scudder, E. C. Sittler, R. B. Torbert, D. Bodet, G. Needell, A. J. Lazarus, J. T. Steinberg, J. H. Tappan, A. Mavretic, and E. Gergin, *Space Sci. Rev.* **71**, 55 (1995).
- [36] R. P. Lepping, M. H. Acuña, L. F. Burlaga, W. M. Farrell, J. A. Slavin, K. H. Schatten, F. Mariani, N. F. Ness, F. M. Neubauer, Y. C. Whang, J. B. Byrnes, R. S. Kennon, P. V. Panetta, J. Scheifele, and E. M. Worley, *Space Sci. Rev.* **71**, 207 (1995).
- [37] R. Bandyopadhyay, A. Chasapis, R. Chhiber, T. N. Parashar, B. A. Maruca, W. H. Matthaeus, S. J. Schwartz, S. Eriksson, O. L. Contel, H. Breuillard, J. L. Burch, T. E. Moore, C. J. Pollock, B. L. Giles, W. R. Paterson, J. Dorelli, D. J. Gershman, R. B. Torbert, C. T. Russell, and R. J. Strangeway, *Astrophys. J.* **866**, 81 (2018).
- [38] M. Dunlop, D. Southwood, K.-H. Glassmeier, and F. Neubauer, *Adv. Space Res.* **8**, 273 (1988).
- [39] L. Franci, P. Hellinger, M. Guarrasi, C. H. K. Chen, E. Papini, A. Verdini, L. Matteini, and S. Landi, *J. Phys. Conf. Ser.* **1031**, 012002 (2018).
- [40] L. Franci, S. Landi, L. Matteini, A. Verdini, and P. Hellinger, *Astrophys. J.* **833**, 91 (2016).
- [41] T. N. Parashar, W. H. Matthaeus, M. A. Shay, and M. Wan, *Astrophys. J.* **811**, 112 (2015).
- [42] W. H. Matthaeus, P. Dmitruk, D. Smith, S. Ghosh, and S. Oughton, *Geophys. Res. Lett.* **30**, 2104 (2003).

- [43] L. Matteini, O. Alexandrova, C. H. K. Chen, and C. Lacombe, *Mon. Not. R. Astron. Soc.* **466**, 945 (2017).
- [44] G. I. Taylor, *Proc. R. Soc. A* **151**, 421 (1935).
- [45] M. Hossain, P. C. Gray, D. H. Pontius, W. H. Matthaeus, and S. Oughton, *Phys. Fluids* **7**, 2886 (1995).
- [46] M. Wan, S. Oughton, S. Servidio, and W. H. Matthaeus, *J. Fluid Mech.* **697**, 296 (2012).
- [47] Y. Yang, W. H. Matthaeus, T. N. Parashar, C. C. Haggerty, V. Roytershteyn, W. Daughton, M. Wan, Y. Shi, and S. Chen, *Phys. Plasmas* **24**, 072306 (2017).
- [48] N. Andrés, F. Sahraoui, S. Galtier, L. Z. Hadid, R. Ferrand, and S. Y. Huang, *Phys. Rev. Lett.* **123**, 245101 (2019).
- [49] See <https://lasp.colorado.edu/mms/sdc/>
- [50] See <https://omniweb.gsfc.nasa.gov/>